



COB-2021-0681

SMALL WIND TURBINE DESIGNED FOR SUPPLYING ELECTRICAL ENERGY TO SMALL HOTELS IN AJURUTEUA-PA-BRAZIL

Mauro J. G. Veloso

Jerson R. P. Vaz

Davi Cavalcante de Oliveira

Antonio M. J. Chaves Neto

Federal University of Pará -Av. Augusto Correa, N. 1 - Belém, PA, 66075-900, Brazil

mauroveloso@ufpa.br, jerson@ufpa.br, davi.cavalcante@ufpa.br, amchaves@ufpa.br

Abstract. *The reduction of greenhouse gas emissions concerns the world. Power plants moved by fossil fuels and their use in industrial processes have generated an incessant search for alternatives, both in energy production and industrial process adjustment, to mitigate the impact on the environment. In this work, the main objective is to show the stages of the design of a small horizontal axis wind turbine to attend an installation of a small hotel in Ajuruteua-PA-Brazil to encourage tourism, generating employment and income for the local population. Also, making it viable by reducing the project operating costs. The rotor blade geometric characteristics were designed by the methodology based on the Blade Element Momentum analysis. The optimization proposed by Glauert is employed, using the corrections proposed by Prandtl and Viteran & Corrigan for the finite number of blades and post-stall behavior, respectively. Wind measurements from the locality were used to estimate the rated wind speed at which the rotor blade was optimized. As a result, an estimative for the starting, aerodynamic torque of the rotor was determined, neglecting the pitch angle adjustment of the blades, as in most small wind turbines, making starting at low wind speed still a severe challenge in the literature.*

Keywords: *Small wind turbines, Starting torque, Turbine optimization, Dynamic modeling Wind turbine.*

1. INTRODUCTION

Climate change has caused constant concerns from governments and research, as well as to development centers for lowering greenhouse gas effect (Schneider, 1989). Researches and development of power plants free from emission are increasing all over the world. Thus, researches have been developed on solar, wind, and tidal energy to optimize projects, lower the installations and operations cost, and increasing operational life (Rueda *et al.*, 2015). In addition, there is the problem of isolated communities dispersed across the vast Amazon region demanding energy to increase their development and improving quality of life. Therefore, researchers are developing studies on energy exploitation (Blanco *et al.* 2008, Quincas *et al.* 2012) through turbine design applied to wind energy (Vaz *et al.*, 2011) and solar energy (Macêdo, 2009).

On the coast of Pará State, a survey of wind potential was carried out by Frade (2000) through a work published in 2000. The study showed the wind statistical distribution data in several Pará coast cities. The data assessed by Frade (2000) on the wind potential of Ajuruteua city was used in the present work. Thus, this paper was proposed to take advantage of the Ajuruteua wind potential to show its technical viability. A turbine was performed by optimized blade based on the Blade Element Momentum Theory (BEMT) (Vaz *et al.*, 2011). The turbine torque starting was evaluated to aid the generator set selection (Ruan *et al.*, 2021). As a result, the turbine starting torque depends on the blade geometry and the aerodynamics characteristics of the airfoil chosen.

2. STARTING TORQUE ESTIMATIVE

At starting, the power generator is off from the turbine powertrain, and the wind energy is concerning to take out the turbine from resting, which means that the turbine rotational speed is zero (Vaz *et al.*, 2018) as further demonstrated in Ruan *et al.* (2021). That leads axial and circumferential inductions factors to vanish, i.e. $a \sim 0$ and $a' \sim 0$, allowing to model the system on a stationary state as in Wood (Wood, 2011). Figure 1 shows the triangle's velocity brief description.

From the blade element theory, the torque (T) and the axial load (F_a) acting on the turbine are given by Eq. (1) and (2).

$$T_r(n) = 0.5\rho_{air}B \int_{r_h}^R c(r)[(2\pi rn)^2 + V_0^2](C_L \sin\phi - C_D \cos\phi)rdr, \quad (1)$$

$$F_a(n) = 0.5\rho_{air}B \int_{r_h}^R c(r)[(2\pi rn)^2 + V_0^2](C_L \cos\phi + C_D \sin\phi)dr, \quad (2)$$

where, ρ_{air} , is the air density at 20°, V_0 , and ϕ are the airflow speed and the flow angle, respectively; C_L , C_D , and $c(r)$, are airfoil lift, drag, and chord, respectively; B , n , and r are the turbine number of blades, rotational speed in rpm and radius form hub, r_h to tip R , respectively.

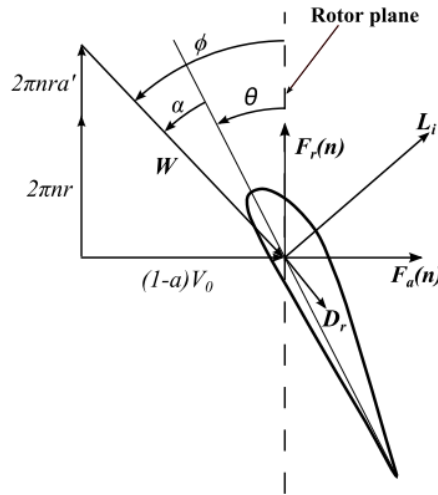


Figure 1. Velocity triangle at a blade section, where “n” is the rotational speed in rpm.

The turbine is considered in imminent rotation, so a and a' vanish. From Fig. 2, it is easy to show that $\phi = 90^\circ$ when $n = 0$, and the angle of attack is given by $\alpha = (90^\circ - \theta)$, where θ is the blade twist angle. So, Eq. (1) and Eq. (2) for starting torque and the axial load becomes, respectively:

$$T_r(n) = 0.5\rho_{air}BV_0^2 \int_{r_h}^R c(r)C_L r dr, \quad (3)$$

$$F_a(n) = 0.5\rho_{air}BV_0^2 \int_{r_h}^R c(r)C_D dr, \quad (4)$$

These equations demonstrate that the torque and axial load depend on the lift and drag coefficients at starting, showing that the angle of attack α is given by $\alpha = (\pi/2 - \theta)$, where θ is the blade twist angle, being an input design parameter for dynamic turbine analyses.

3. METHODOLOGY

It is essential to know the average energy consumption for the low-cost hotel, which was evaluated and showed to be of 240 kWh/day. This value was assessed considering the number of commercial kitchen equipment and other electrical devices applied to the hotel and the respective energy consumption. All these consumption rates are available on the table for household consumptions, published by INMETRO (INMETRO, 2020), and the equipment datasheet is acquirable from the manufacturer. However, it is important to know that the hotel's higher demand is in July and holidays. Lower demands occur on other days of the year. These realities decrease the annual average energy consumption.

The turbine rotor was designed using the approach described in Vaz *et al.* (2011). The wind velocity was based on the measurements and data processed by Frade (2000). These data has been shown that the wind speed is from 6.19 to 10.01 m/s range in Ajuruteua beach for higher probability density function.

In the work of Frade (2000), the wind probability density function of Weibull distribution for measurements made in Ajuruteua beach from 1996 to 1998 showed that the high value for the wind speed distribution was 8.5 m/s. Thus, this was the design wind speed value applied to the turbine optimization.

In Tab. 1, the parameters to design the turbine blades are shown. Table 2 shows the turbine design parameters and some necessary considerations. First, the Turbine power was chosen considering a small wind turbine manufacturer, a

commercial neodymium generator of 1500 W at 210 RPM, and a nominal power turbine design of 2300 W, accounting for all dissipative effects.

Equations (3) and (4) were numerically evaluated by MatLab™ scrips after geometric optimum blade design, for each NACA (Airfoils Tools, 2020) airfoil parameter (Vaz *et al.*, 2011). Therefore, for each airfoil, it is assigned a different optimized blade shape. From Tab. 1, it is noted that NACA 6043 has the biggest CL/CD ratio.

Table 1. Design parameters.

Airfoil	Design Parameters ⁽¹⁾				
	Angle		Coefficients (Design)		
	Attack (design)	Stall	CL	CD	CL/CD
NACA 4412	5.5°	15°	1.0652	0.00997	109.8144
NACA 4414	5.0°	15°	1.0049	0.01042	96.4395
NACA 6040	6.0°	15°	1.0122	0.01056	95.8523
NACA 6042	2.75°	15°	0.8218	0.00671	122.4739
NACA 6043	3.0°	15°	1.0761	0.00757	142.1532
NACA 653618	6.0°	7.5°	1.1590	0.01078	107.5139

⁽¹⁾ all the design parameters account for 500,000 Reynolds numbers.

⁽²⁾ source (Airfoils Tools, 2000).

Table 2: Wind turbine parameters design data

Parameter	Values
Radius hub	0.1D _{turbine}
Number of blades	3
Air density ⁽¹⁾	1.226 kg/m ³
Sound speed	340 m/s
Dynamic viscosity	1.818x10 ⁻⁵ N.s/m ²
Power Coefficient (Cp)	0.45
Turbine rotation speed	210 RPM
Minimum wind speed	3.0 m/s
Maximum wind speed.	12.5 m/s
Tol.	0.001

⁽¹⁾ measured at 25°C

4. RESULTS AND DISCUSSION

This section presents the results and discussion of the paper. Figure 2 shows the chord length distribution over the radial rotor dimension. Such a distribution indicates that the starting torque from the rest is significant for the small wind turbine, as an increased chord usually leads to an increased torque (Ruan *et al.*, 2021).

The chord and twist angles of designed turbine blades in Figs. 2 and 3 were compatible with the technical literature available, as shown in the work of El-Okda (2015). In this case, NACA 653618 has the most significant chord distribution along the blade length.

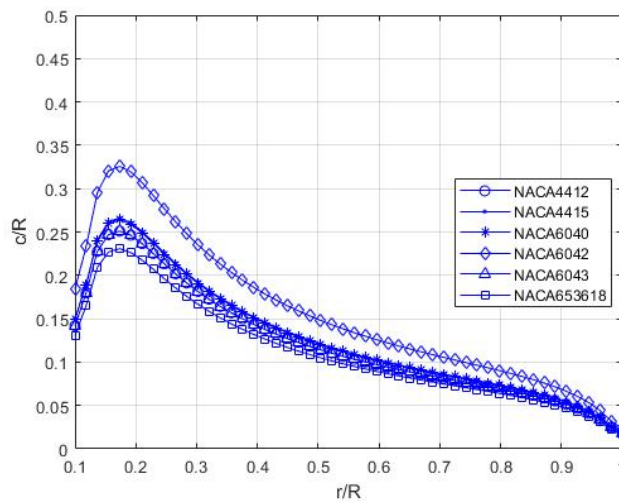


Figure 2. Ratio chord/R for various airfoils turbine blades.

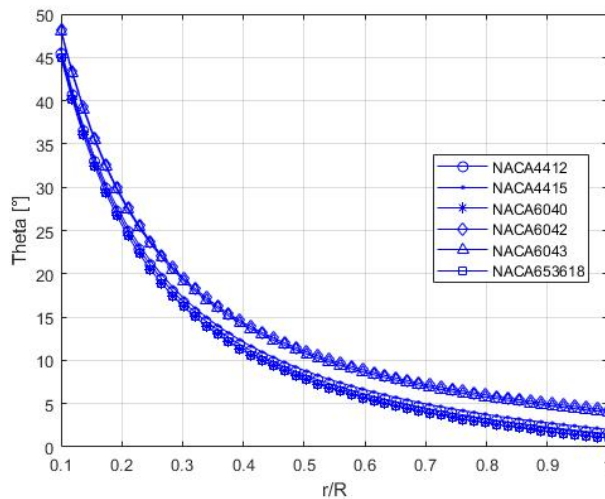


Figure 3. Twist angle of the turbine blades designed.

Figure 4 depicts the axial and tangential load; the latter is essential to starting torque and nominal operation, so the higher lift load at stationary state is better for starting torque magnitude. In addition, the axial load values are important to evaluate the dissipative torque at the starting turbine, as they are included in the calculation of the resistance torque imposed by the turbine powertrain. This analysis allows the calculation of the minimum wind speed to generate electrical power. Regarding the turbine powertrain analysis, it is not included in the present work.

Figure 5 shows the estimating starting torque for typical airfoils, displaying that the estimated values were tiny at low wind speed values. Furthermore, the estimated starting torque turbine for 3.5 m/s wind speed was 9.9 Nm, higher than 6.25 Nm at 3.0 m/s wind speed, the minimum torque at threshold electrical power energy.

Table 3 shows the turbine's design values, axial and starting torque for 3.0 m/s wind speed. Figure 5 depicts that for 3.5 m/s wind velocity, the starting torque is 9.9 Nm, which is also greater than 6.25 Nm for a 1.5 kW 72V commercial neodyme generator available in Brazil. Thus, for 3.5 m/s wind velocity, the set turbo-generator designed starts to generate electricity. For all airfoil applied in the turbine design, the starting torque output evaluated is slightly different; the maximum observed difference was about 4.0 Nm for 8.5 m/s wind speed.

In Tab. 3, it was shown that the greater starting torque depends on the product of C_L values by blade-area ratio, even great values of c/R do not imply excellent starting torque, as depicted in Fig. 2. The best turbine starting torque needs to be measured in terms of products between C_L and blade-area ratio, as described in Tab. 3. So then, higher C_L/C_D needs to be considered as an excellent parameter to aid airfoil blade selection, as also supported by the work of El-Okda (2015).

Table 3. Design turbine blades for various airfoils

AIRFOIL	Blade-area ratio	Blade Length	Axial Load	CLxBlade-area ratio	Starting Torque (Nm)
NACA 4412	0.1042	2.0789	0.0802	0.1110	7.2792
NACA 4415	0.1104	2.0789	0.0862	0.1110	7.2771
NACA 6040	0.1096	2.0789	0.0867	0.1110	7.2769
NACA 6042	0.1351	2.0789	0.0679	0.1111	7.2817
NACA 6043	0.1042	2.0789	0.0585	0.1120	7.3454
NACA 653618	0.0958	2.0789	0.0773	0.1110	7.2793

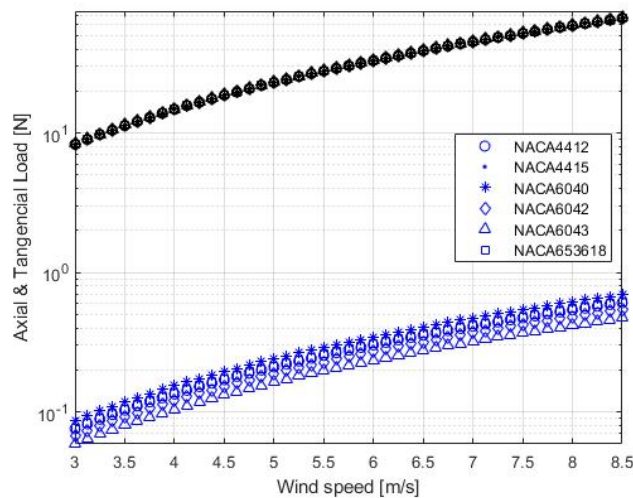


Figure 4. Axial and tangential starting forces versus wind speed. Axial load values, in blue, are below 0.1N, and tangential is 100 times high for 3 m/s wind speed.

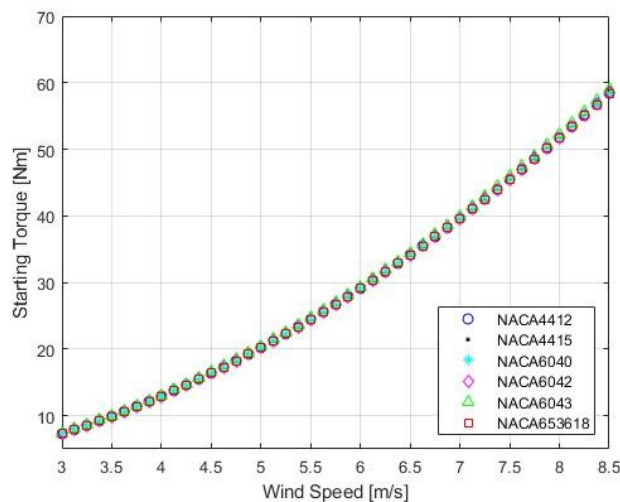


Figure 5. Estimating starting torque for different wind speeds.

Thus, as Vaz *et al.* (2018) mentioned, the lowest axial force has the lowest dissipative torque. So, higher starting torque (starting torque = starting torque - dissipative friction torque at imminent rotating turbine) is a crucial parameter in turbine design.

5. CONCLUSIONS

This article showed different optimized small HWAT designs for small hotels in Ajuruteua-PA-Brazil. The BEMT model was used to design the optimized blade geometry and the starting torque. The increased optimum chord and twist angle contribute to an increase in the starting torque of the turbine, but they are not enough. So, the turbine starting torque depends on the blade geometry and the aerodynamics characteristics of the airfoil chosen. The best starting turbine torque needs to be measured in terms of product between lift coefficient and blade-area ratio, as shown in Tab. 3. Even though the present work does not consider the turbine dynamic behavior, these results are essential to turbine dynamic characteristics, improving the design of turbine powertrains. This is because, according to Vaz *et al.* (2018), the drivetrain torque is dominated by the resistance of the bearings as opposed to the much larger generator torque that would occur during power extraction. An accurate formulation for the static frictional torque allows an accurate estimation of the starting wind speed for a turbine. They noted that the starting wind speed of a small turbine may be much higher than the cut-in wind speed. The combination of accurate drivetrain resistance and low speed rotor aerodynamic models have the potential for optimization of turbine design to significantly reduce the starting wind speed and increase the operating range of high efficiency.

6. ACKNOWLEDGEMENTS

The authors would like to thank the CNPq, PROCAD/CAPES (Agreement: 88881.200549/2018-01), and PROPESP/UFPA for financial support.

7. REFERENCES

- Airfoils Tools, 2020. *Airfoils Tools (web publications)*, <http://airfoiltools.com/search/index?m%5BmaxCamber%5D=0&m%5Bsort%5D=5>. Accessed 19 September 20.
- Blanco, C. J. C., Mesquita, A. L. A., 2008. "Decision support system for micro-hydropower plants in the Amazon region under a sustainable development perspective", *Energy for Sustainable Development*, Volume XII No. 3, pp. 13 – 21.
- El-Okda, Y. M., 2015, "Design methods of horizontal axis wind turbine rotor blades", *Int. J. Industrial Electronics and Drives*, Vol. 2, No. 3, pp 135 – 150.
- Farias, G. M., Galhardo, M. A., Vaz, J. R., Pinho, J. T., 2019. "A steady-state based model applied to small wind turbines". *Journal of the Brazilian Society of Mechanical Sciences and Engineering*, Vol. 41, No. 5, pp. 1-10.
- Frade, L. C., 2000. "Study of the Wind Energy Potential on the Coast of the State of Para" (in Portuguese), Master's Dissertation, Graduate Program in Electrical Engineering, Federal University of Pará, Belém, Brazil.
- INMETRO, 2020. *INMETRO households energy consumption table (web publication)*. National Institute of Metrology, Standardization and Industrial Quality (INMETRO), <http://www.inmetro.gov.br/consumidor/tabelas.asp>. Accessed 2 September 2020.
- Lopes, J.J.A. , Vaz, J.R.P. , Mesquita, A.L.A., Mesquita, A.L.A., Blanco, C.J.C., 2015. "An Approach for the Dynamic Behavior of Hydrokinetic Turbines", *Energy Procedia* Vol. 75, pp. 271-276.
- Mesquita, A.L.A. Mesquita, A.L.A., Palheta, F.C. , Vaz, J.R.P. , Morais, M.V.G. , Goncalves, C., 2014. "A methodology for the transient behavior of horizontal axis hydrokinetic turbines". *Energy Conversion and Management*, Vol. 87, pp. 1261-1268.
- Macêdo, W. N., Zilles, R., 2009. "Influence of the Power Contribution of a Grid Connected Photovoltaic System and its Operational Particularities". *Energy for Sustainable Development*, Vol. nº 13, pp 202-211.
- Moreira, J.L.R., Mesquita, A.L.A., Araujo, L.F., Galhardo, M.A.B., Vaz, J.R.P., Pinho, J.T., 2020. "Experimental investigation of drivetrain resistance applied to small wind turbines". *Renewable Energy*, Vol. 153, pp. 324-333.
- Quintas, M. C., Blanco, C. J. C, Mesquita, A. L.A., 2012. "Analysis of two schemes using micro-hydroelectric power (MHPs) in the Amazon with environmental sustainability and energy and economic feasibility". *Environment, Development, and Sustainability*, Vol. 14, No. 2, pp 283-294.
- Ruan S. R., Rio Vaz Deborah A.T.D., Vaz, Jerson R.P., "The generalized Maxwell-slip friction model applied to start of small wind turbine". *Journal of the Brazilian Society of Mechanical Sciences and Engineering*, Vol. 43, No. 376.
- Rueda, S. A. J., and Vaz, J. R. P., 2015. "An approach for the transient behavior of horizontal axis Wind turbines using the blade element theory", *Ciência & Engenharia (Science & Engineering Journal)*, Vol. 24, No.2, pp. 95 – 102.
- Schneider, S. H., 1989. "The greenhouse effect: Science and policy". *Science*, 243: 771 - 781.
- Vaz, J. R. P., Pinho, J.T., and Mesquita, A.L.A., 2011. "An extension of BEM method applied to horizontal-axis wind turbine design". *Renewable Energy*, Vol. 36, Issue 6, pp. 1734-1740.
- Vaz, J.R.P., Wood, D.H. , Bhattacharjee, D. , and Lins, E.F., 2018. "Drivetrain resistance and starting performance of a small wind turbine". *Renewable Energy*, Vol. 117, pp. 509-519.
- Wood, D.H., 2011. "Small Wind Turbines: Analysis, Design, and Application". Ed. Springer-Verlag, London.

8. RESPONSIBILITY NOTICE

The authors are the only ones responsible for the printed material included in this paper.